

BitDecoding: Unlocking Tensor Cores for Long-Context LLMs Decoding with Low-Bit KV Cache

Dayou Du*
University of Edinburgh
dayou.du@ed.ac.uk

Shijie Cao†
Microsoft Research
shijiecao@microsoft.com

Jianyi Cheng
University of Edinburgh
jianyi.cheng@ed.ac.uk

Ting Cao
Microsoft Research
ting.cao@microsoft.com

Mao Yang
Microsoft Research
maoyang@microsoft.com

Abstract

The growing adoption of *long-context* Large Language Models (LLMs) has introduced significant memory and computational challenges in autoregressive decoding due to the expanding *Key-Value (KV) cache*. KV cache quantization has emerged as a promising solution, with prior work showing that 4-bit or even 2-bit quantization can maintain model accuracy while reducing memory costs. However, despite these benefits, preliminary implementations for the low-bit KV cache struggle to deliver the expected speedup due to quantization and dequantization overheads and the lack of Tensor Cores utilization. In this work, we propose **BitDecoding**, a GPU-optimized framework that unlocks Tensor Cores for efficient decoding with low-bit KV cache. Efficiently leveraging Tensor Cores for low-bit KV cache is challenging due to the dynamic nature of KV cache generation at each decoding step. BitDecoding addresses these challenges with a Tensor Cores-Centric BitFusion Scheme that ensures data layout compatibility to enable high utilization of Tensor Cores. Additionally, BitDecoding incorporates a warp-efficient parallel decoding kernel and a fine-grained asynchronous pipeline, minimizing dequantization overhead and improving computational efficiency. Experiments show that BitDecoding achieves up to 7.5× speedup on RTX 4090, 4.8× on A100, and 8.9× on H100, compared to FP16 FlashDecoding-v2. It also outperforms the state-of-the-art low-bit KV cache implementation (QServe) by up to 4.3×. On LLaMA-3.1-8B with a 128K sequence length, BitDecoding reduces single-batch decoding latency by 3×, demonstrating its effectiveness in long-context generation scenarios. The code is available at <https://github.com/DD-DuDa/BitDecoding>.

1 Introduction

The ability of Large Language Models (LLMs) to process long contexts [8, 23, 29] has unlocked new capabilities, such as book summarization [4], multi-modal understanding [34], and test-time scaling [10, 22]. However, these advancements come with significant memory and computational challenges, primarily due to the large size of the Key-Value (KV) cache

in long-context scenarios. During autoregressive decoding, LLMs must repeatedly access this growing cache for each generated token, which increases memory usage and slows down decoding. The problem worsens with larger batch sizes, as the KV cache scales linearly with the number of concurrent queries. For example, a 7B model requires approximately 14GB GPU memory for its parameters, but with a 32K context length and a batch size of 8, the KV cache alone consumes 128GB GPU memory [12], creating a significant memory bottleneck.

To address this growing bottleneck, KV cache quantization has emerged as a promising solution. By reducing the bit-width of the KV cache, quantization lowers memory overhead and improves overall efficiency. Recent quantization algorithms have shown that low-bit KV cache can retain high accuracy. QServe [18] demonstrates 4-bit KV cache improves throughput on models like LLaMA-3 and Qwen-1.5 while maintaining strong accuracy, even together with 4-bit weight and 8-bit activation. Further research [14, 19, 27] shows that 2-bit KV cache can achieve near fp16 accuracy. KIVI [19], for instance, incurs only a 0.6% accuracy drop on LongBench [3] with a 2-bit KV cache on LLaMA-2-7B-Chat. Recent studies [28, 36] explore 1-bit quantization for KV cache, maintaining acceptable accuracy under specific conditions. These results confirm that KV cache quantization strikes an effective balance between efficiency and accuracy, making it viable for long-context LLM deployment.

Despite the memory savings, current system support for low-bit KV cache struggles to deliver the expected speedup. Previous implementations [18, 19, 37] remain preliminary and case-specific, with significant room for further systematic optimization. A major bottleneck lies in the overhead introduced by quantization and dequantization. Although the KV cache is low-bit, the query (Q) values and attention scores remain in high precision. This results in mixed-precision matrix multiplications (mpGEMM), which existing hardware does not natively support, requiring dequantization before multiplication. Previous mpGEMM kernels like Ladder [32] and Marlin [9] are designed for low-bit weights but cannot be directly applied to low-bit KV caches. This is because weights are static and stored offline, while KV caches are

*Work done during the internship at Microsoft Research.

†Corresponding Author.

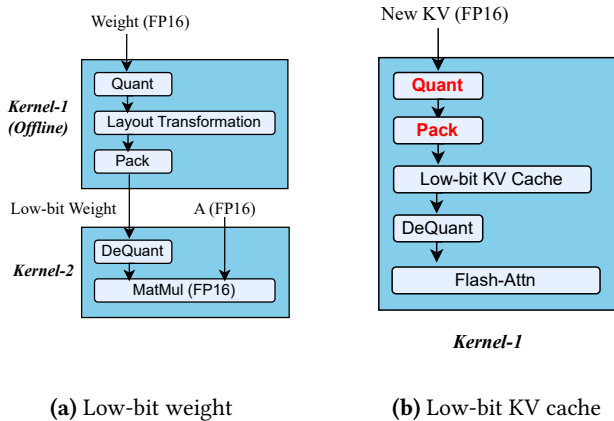


Figure 1. Comparison of mixed-precision matrix multiplication for low-bit weight and low-bit KV cache. (a) Quantized weights can be preprocessed offline. (b) KV cache requires online quantization and packing for each newly generated token.

dynamic and generated online. In autoregressive decoding, each newly generated token requires quantization, packing, and dequantization of the low-bit KV cache, introducing significant overhead and complexity in GPU kernel design, as illustrated in Figure 1.

To address this, our insight is to leverage Tensor Cores for intensive matrix multiplications while efficiently utilizing CUDA cores for KV cache dequantization. Previous work has relied solely on CUDA cores, leaving Tensor Cores underutilized, as shown in Table 1. Our approach is based on three key observations: First, modern language models employ Grouped-Query Attention (GQA) and Multi-Query Attention (MQA), which share a group of keys across multiple queries, enabling Tensor Cores to accelerate dot products in the self-attention mechanism. Second, leveraging Tensor Cores can alleviate computational pressure on CUDA cores, enabling more efficient execution of dequantization. Finally, newer GPU architectures like Hopper support asynchronous execution on Tensor Cores [20], allowing the extra operations introduced by the low-bit KV cache to overlap with computation, further enhancing efficiency.

However, efficiently leveraging Tensor Cores for decoding with low-bit KV cache presents significant challenges due to the dynamic nature of KV cache generation at each decoding step. First, Tensor Cores have a rigid computation layout, requiring low-bit packed data to be dequantized and aligned with higher-precision formats. This is challenging in autoregressive decoding, where the KV cache dynamically expands and the dequantized data must conform to Tensor Core-specific layouts. Second, the high computational cost of dequantization might stall computations on Tensor Cores, reducing GPU occupancy and leading to poor hardware utilization. This mismatch between dequantization on CUDA

Table 1. Comparison of low-bit KV cache system implementation. BitDecoding improves generality by supporting Tensor Cores (TCs), per-channel (K-C) and per-token (K-T) quantization for Key Tensor, and FlashAttention-3 [25] for enhanced efficiency on Hopper GPU.

Method	Serving	Quant	Bit	FA.	TCs.
KIVI [19]	Single	K-C	4,2	-	-
Atom [37]	Page	K-T	4	FA2	-
QServe [37]	Page	K-T	4	FA2	-
BitDecoding	Single, Page	K-C, K-T	4,2	FA2, FA3	✓

cores and matrix multiplication on Tensor Cores might create a significant bottleneck in decoding efficiency.

To bridge this gap, we propose **BitDecoding**, a GPU system design optimized for low-bit KV cache with unified Tensor Cores support for varying bit-widths and scaling directions (per-token and per-channel). To resolve layout mismatch, we introduce a *Tensor Cores-Centric BitFusion Scheme* that enables efficient warp-level quantization and packing, ensuring compatibility with Tensor Core layouts and accelerating dequantization using faster instructions. Additionally, we develop *Warps-Efficient Parallel Dequantization* which reduces dequantization overhead by using a shared memory buffer to enhance warp-level parallelism beyond traditional flash attention. Finally, we design an efficient pipeline that enables seamless cooperation between CUDA cores, Tensor Cores, and the GPU memory hierarchy, while leveraging the asynchronous execution on newer GPU architectures to enhance performance.

We evaluate the performance of BitDecoding at both the kernel level and the end-to-end model level, comparing it with FP16 FlashDecoding-v2 and other implementations such as KIVI, Atom, and Qserve. At the kernel level, our evaluation shows that BitDecoding achieves up to 7.5 \times speedup on RTX 4090, 4.8 \times on A100, and 8.9 \times on H100. Additionally, it outperforms the state-of-the-art low-bit KV cache implementation, Qserve, by up to 4.3 \times . At the end-to-end model level, BitDecoding reduces single-batch decoding latency by 3 \times on LLaMA-3.1-8B with a 128K sequence length and achieves over 4 \times higher serving throughput than Qserve.

2 Background

2.1 LLM Inference

LLMs, built on the transformer architecture [31], rely on self-attention to model token relationships. During inference, they operate in two phases: (i) Prefill, where the input prompt is processed to generate the KV cache, and (ii) Decode, where the KV cache is updated token by token to generate new outputs.

Prefill Phase. Consider an input prompt of length L . The Query (Q), Key (K), and Value (V) tensors are computed

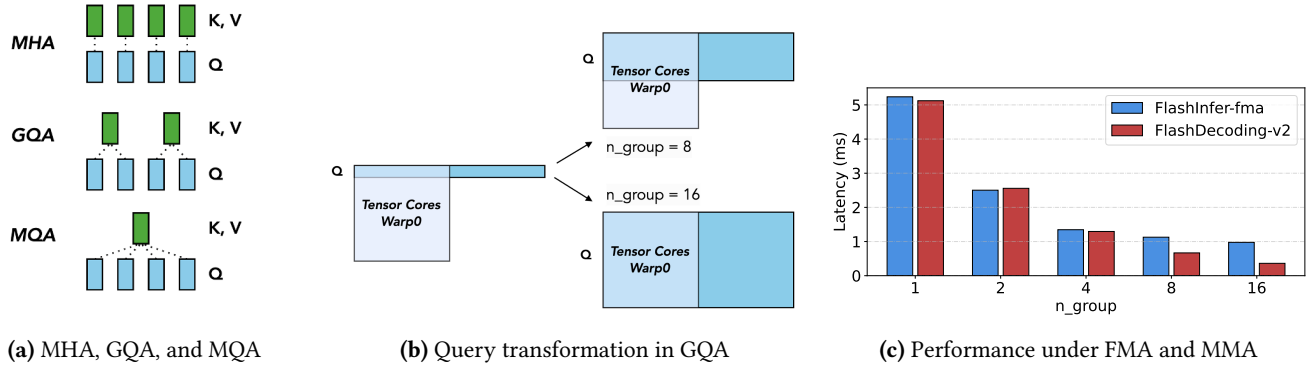


Figure 2. GQA and MQA improve Tensor Cores utilization as n_group increases, where $n_group = \frac{head_q}{head_{kv}}$.

via linear projections. The shapes of K and V are given by $K, V \in \mathbb{R}^{b \times L \times h_{kv} \times d}$, where b is the batch size, h_{kv} is the number of KV heads, and d is the hidden size. Once computed, the KV tensors are cached in memory to facilitate efficient decoding.

Decode Phase. For each new token, the model generates new tensors $Q \in \mathbb{R}^{b \times 1 \times h_q \times d}$, $K_{new}, V_{new} \in \mathbb{R}^{b \times 1 \times h_{kv} \times d}$, and updates the KV cache:

$$\begin{aligned} K &\leftarrow \text{Concat}(K, K_{new}), \\ V &\leftarrow \text{Concat}(V, V_{new}). \end{aligned} \quad (1)$$

The attention output is then computed as:

$$O = \text{Softmax}\left(\frac{QK^T}{\sqrt{d}}\right)V, \quad (2)$$

FlashAttention. Full attention has $O(L^2)$ complexity in both computation and memory. FlashAttention [6] mitigates this via block-wise tiling and strategic recomputation. It processes input matrices $Q \in \mathbb{R}^{T_m \times d}$, $K, V \in \mathbb{R}^{T_n \times d}$ in tiles within shared memory, using block sizes T_m and T_n . The number of key-value tiles is $C_n = \lceil L/T_n \rceil$. For each key-value tile $j \in [0, C_n)$, the computation follows Algorithm 1. Building on FlashAttention, FlashDecoding [7] enhances GPU performance for long-context autoregressive decoding via fixed-split partitioning and a reduce-combine kernel.

Algorithm 1 FlashAttention Computation on chip

- 1: $S = QK_j^T$, where $S \in \mathbb{R}^{T_m \times T_n}$.
 - 2: $m^{new} = \max(S, \text{rowmax}(S))$.
 - 3: $P = \exp(S - m^{new})$, where $P \in \mathbb{R}^{T_m \times T_n}$.
 - 4: $O^{new} = PV_j + \text{diag}(e^{m - m^{new}})O$.
-

2.2 KV Cache Quantization

The process of KV cache quantization and dequantization using B-bit integer representation can be formulated as:

$$X_q = \left\lfloor \frac{X - \text{zeros}}{\text{scale}} \right\rfloor, \quad (3)$$

$$X_{dq} = FP_{\text{convert}}(X_q) \cdot \text{scale} + \text{zeros}$$

where $\text{zeros} = \min X$ is the zero-point, $\text{scale} = \frac{\max X - \min X}{2^B - 1}$ is the scaling factor, and $\lfloor \cdot \rfloor$ denotes the rounding operation. The quantized values X_q are packed into higher-precision integer storage, reducing the data memory loading by a factor of $(16/B) \times$ in half-precision computing.

KV cache tensors can be quantized along either the token or channel dimensions in a group-wise manner. Specifically, for $K, V \in \mathbb{R}^{T_n \times d}$, token-wise quantization operates along the d dimension, whereas channel-wise quantization is applied along the T_n dimension.

3 Opportunities and Challenges

3.1 Opportunities of Leveraging Tensor Cores

Despite the growing demand for low-bit KV caches, there is presently no system available that facilitates Tensor Cores computation for this purpose. In this section, we highlight the important role of Tensor Cores in modern LLMs attention structures and GPU architectures and demonstrate their advantages in mixed-precision computing for low-bit KV cache decoding.

Enable GQA and MQA Acceleration. Modern attention mechanisms, such as Grouped-Query Attention (GQA) [2] and Multiple-Query Attention (MQA) [26], leverage Tensor Cores to enhance decoding efficiency by improving computational throughput. As shown in Figure 2a, the grouping factor is defined as:

$$n_group = \frac{head_q}{head_{kv}} \quad (4)$$

where $n_group > 1$ in GQA, and $head_{kv} = 1$ in MQA. As shown in Figure 2b, since multiple query heads share the same KV, the query tensor can be transformed to enlarge the

Q tile, maximizing Tensor Cores warps utilization as follows:

$$[1, (n_group, head_kv)] \rightarrow [n_group, head_kv] \quad (5)$$

This restructuring enhances parallelism and significantly boosts Tensor Cores efficiency. Performance results in Figure 2c demonstrate substantial speedups as n_group increases, outperforming CUDA cores-only computation.

Enable FlashAttention-3 with Hopper Tensor Cores.

The Hopper architecture introduces SM90 Tensor Core instructions supporting warp-specialized pipeline, delivering up to $6\times$ decoding speedup over previous implementations while relying solely on mma instructions reduces peak throughput by 35% [25]. Extending low-bit KV cache decoding compatibility with FlashAttention-3 can leverage optimized warp group-level scheduling and asynchronous execution for further efficiency and throughput improvements.

Reduce Computational Pressure on CUDA Cores. In mixed-precision computation, CUDA cores typically handle costly dequantization tasks, including data-type conversions and element-wise operations, consuming substantial processing power. Previous implementations like Atom and QServe relied entirely on CUDA cores for both dequantization and matrix multiplication, causing high computational overhead. Offloading matrix multiplication to Tensor Cores reduces this burden, enabling CUDA cores to focus solely on dequantization. This separation optimizes workload distribution, enhances warp scheduling, and improves overall hardware utilization.

3.2 Challenges in Tensor Cores Utilization

Given the opportunities in Section 3.1, designing a unified system supporting low-bit KV Cache with efficient Tensor Core utilization remains challenging due to the dynamic KV cache expansion. On one hand, enabling Tensor Cores is complicated by their rigid computation layout, requiring aligned dequantization from low-bit to higher-precision formats. On the other hand, the high overhead of dequantization further limits efficient GPU utilization without fine-grained kernel optimization.

Layout Mismatch between Quant and Dequant. Aligning data layouts for Tensor Cores computation is challenging, especially in autoregressive generation with dynamically expanding KV caches. After quantization and packing, KV cache must match the FP16 layout during dequantization. Existing static-weight layout transformations are unsuitable for this dynamic context [9, 11, 32].

In Tensor Core operations, threads load data from shared memory into registers following a fixed yet complex pattern, determined by instructions like `mma.m16n8k16` and `mma.m8n8k8`. As illustrated in Figure 3, accurately dequantizing low-bit packed data within registers to match Tensor Cores’ layout requirements remains particularly difficult.

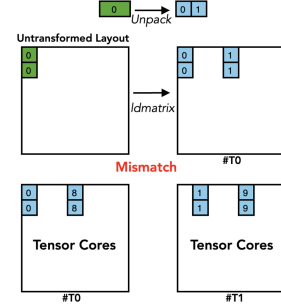


Figure 3. Packing Layout Mismatch because of the interleaved pattern on Tensor Cores.

Dequantization Limits Tensor Cores Utilization. Under FlashAttention’s original warp partitioning, the computational overhead of dequantization significantly reduces performance and Tensor Core utilization.

As shown in Figure 4a, FlashAttention assigns a single warp along the N dimension for register-level softmax and matrix multiplication (PV), with P stored in registers aligned to Tensor Core layouts. However, this approach becomes inefficient when extra dequantization operations require small warp tiles in K or V to sequentially traverse the N dimension. Frequent dequantization stalls Tensor Cores, lowering GPU occupancy and hardware efficiency.

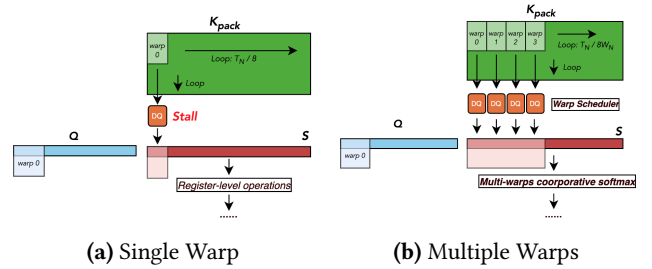


Figure 4. (a) A single warp along N for register-level operations will experience stalls due to dequantization (DQ) (b) Warps-Efficient Parallel Dequantization (see Section 4.2).

4 BitDecoding

BitDecoding is a high-performance, GPU-optimized system designed to accelerate LLMs decoding with a low-bit KV cache. To address the challenge of layout mismatch, we propose a Tensor Cores-Centric BitFusion Scheme that ensures data layout compatibility, enabling Tensor Cores utilization (Section 4.1). To mitigate low computational utilization caused by the extreme overhead of dequantization, we introduce a warp-efficient design (Section 4.2) and illustrate our fine-grained, asynchronous software pipeline (Section 4.3),

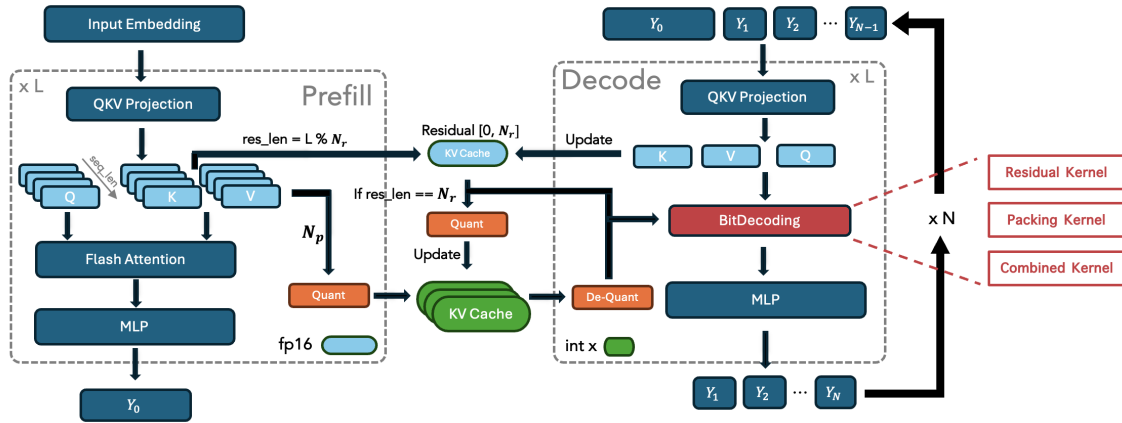


Figure 5. Overview of the BitFusion System. The system introduces an fp16 residual KV cache, managed by a Residual Kernel that fuses quantization and a Packing Kernel efficiently processes the low-bit packed KV cache with efficient dequantization.

where computing units and the GPU memory hierarchy collaborate for mixed-precision computation under the FlashAttention mechanism.

4.1 Tensor Cores-Centric BitFusion Scheme

4.1.1 BitFusion System overview. As illustrated in Figure 5, after the prefill phase, the majority of the KV cache is quantized into a Tensor Cores-friendly layout and stored in low-bit packing storage, while a smaller portion is preserved in high-precision within the residual KV cache. To achieve efficient execution, BitDecoding launches two specialized GPU kernels that fuse low-bit operations and one combined kernel for reduction:

1. **Residual Kernel (half precision):** This kernel processes the residual KV cache, performing both quantization and packing fusion.
2. **Packing Kernel (low bit):** This kernel handles the low-bit packing KV cache, leveraging Tensor Cores with efficient dequantization.
3. **Combined Kernel:** This kernel combine the result from the residual kernel and multiple splits output from the packing kernel.

The introduction of residual KV Cache enables on-the-fly quantization fused directly into the attention operation and also provides flexible granularity, supporting both token-wise and channel-wise quantization [19].

Tensor Cores-Centric Design. As shown in Figure 6, this design ensures that the low-bit packed data generated by the *Residual Kernel* can be correctly unpacked for Tensor Cores computations in the *Packing Kernel*. Specifically, two kernels must share the same `ldmatrix` instruction under a consistent `mma` warp layout, such as `ldmatrix.x2` and `mma.m16n8k16` with a specific warp tiling pattern.

In the *Residual Kernel*, the packed data stored in registers is inherently structured according to the `ldmatrix` loading instruction, ensuring alignment with the Tensor Cores data layout. This guarantees that low-bit packed data is arranged in the interleaved format required by Tensor Cores. In the *Packing Kernel*, the packed data is unpacked while preserving register alignment for Tensor Cores computations.

This structural alignment allows the residual KV block to naturally pair quantization and dequantization layouts with Tensor Cores-specific instructions.

Residual Block Size. Due to the interleaved pattern of the Tensor Cores layout, the residual block size N_r in the *Residual Kernel* is determined based on the Tensor Cores warp tiling layout. Given the PTX-level instruction `mma.m16n8k16` and warp-level tiling along the N dimension (denoted as W_n), we adopt an INT16 storage format. The corresponding N_r is computed as:

$$\text{pack_num} = \frac{16}{\text{num_bits}}, \quad (6)$$

$$N_r = 8 \times W_n \times \text{pack_num}.$$

Figure 7 demonstrates why $N_r = 16$ when $\text{num_bit} = 8$ with an example of how the data processed by Thread 0 (T0) is quantized and packed into smaller slices.

BitDecoding Inference Execution Flow. Algorithm 2 outlines the modified LLMs inference flow introduced by the residual KV cache and the *Residual Kernel*. During inference, KV cache entries are divided into quantized and residual (unquantized) segments. The residual cache size is determined by $L\%N_r$ for Tensor Core alignment. In the Decoding phase, attention for the residual segment is computed by the *Residual Kernel*, followed by the quantized cache using the *Packing Kernel*. The results are combined using the *Combine Kernel*, similar to FlashDecoding. The Cache Update phase

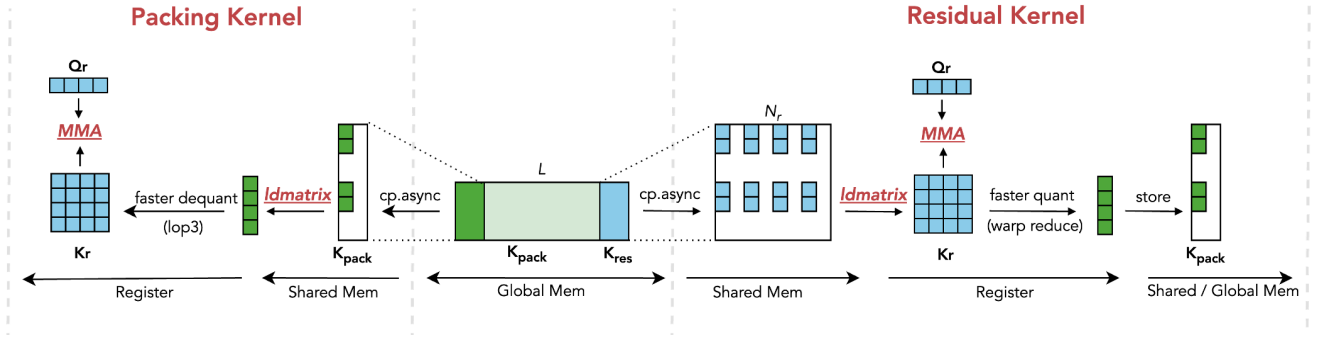


Figure 6. Tensor Cores-Centric Design. The Residual kernel and the Packing Kernel share the same `ldmatrix` and `mma` to enable low-bit data layout compatibility.

integrates newly quantized entries into the packed cache for subsequent inference steps.

4.1.2 Residual Kernel for Quantization. As shown in Figure 7, the *Residual Kernel* efficiently computes quantization parameters and performs packing with minimal overhead.

Quantization involves reductions and element-wise transformations, introducing runtime overhead. To efficiently compute scale and zero-point values, we first apply thread-level reduction, followed by warp-level reduction using the PTX instruction `__shfl_xor_sync` to aggregate values within warps. When the warp repetition factor $W_n > 1$, a small shared memory buffer enables communication across warps.

After calculating quantization parameters, data undergoes register-level quantization before packing into INT16 storage. Additionally, we use `half2` to compactly store both scale and zeros, optimizing memory access and computation during dequantization.

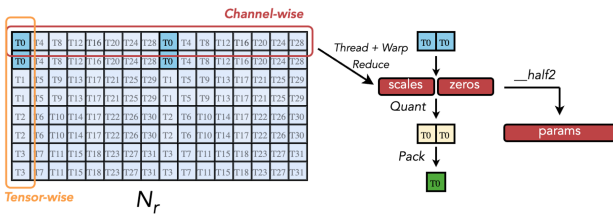


Figure 7. Example of Quantization and Packing. (1) As the thread spacing is 8, $N_r = 16$ when using INT16 to pack two INT8 values. (2) The quantization parameters are computed within each warp.

4.1.3 Packing Kernel for Dequantization. As shown in Figure 8, the *Packing Kernel* employs a faster dequantization mapping based on low-level bitwise operations and instructions inspired by [15].

Directly casting low-bit values to FP16 using `static_cast` introduces significant overhead. To mitigate this inefficiency,

we first load INT16-packed data into registers using `ldmatrix`, then cast them to INT32 before mapping them to the interleaved Tensor Core layout following the 75316420 pattern. This layout enables efficient conversion of INT4/INT2 data to FP16 using the `lop3` instruction for bitwise manipulation while aligning with the Tensor Core computation pattern.

Additionally, since we store quantization parameters in `half2` format, we further optimize dequantization by leveraging the `__hfm2` instruction, enabling efficient fused multiply-add operations during transformation.

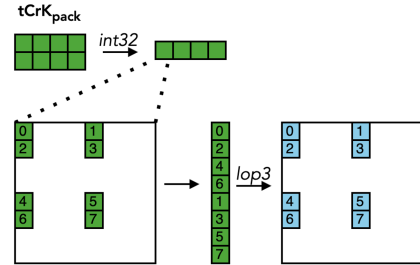


Figure 8. Faster Dequantization Mapping. We use the `lop3` instruction instead of inefficient `static_cast`, following interleaved pattern on Tensor Cores.

4.1.4 Hopper Tensor Cores Optimization. We optimize the *Packing Kernel* for Hopper Tensor Cores by efficiently managing low-bit quantized data within Warpgroup Matrix Multiply-Accumulate (WGMMMA) constraints, integrating seamlessly with Hopper’s asynchronous execution.

WGMMMA imposes a key constraint: in a matrix multiplication $C = AB$, only A and C can be sourced from registers, while B must reside in shared memory. This presents a challenge for low-bit quantized data, as values are typically upconverted to FP16 in registers before computation. To resolve this, we employ Hopper’s STSM PTX instruction to store dequantized FP16 values in shared memory efficiently, accessible for `wgmma_SS` operations. Remarkably, the

Algorithm 2 BitDecoding Inference Execution Flow

```

1: function PREFILL
2:   Input: kv_cache, Context_Len L, Nr
3:   % ... After computation ...
4:   kv_cache_pack ← [ ], kv_cache_residual ← [ ]
5:   res_len ← L mod Nr
6:   Np ← L - res_len
7:   kv_pack ← qpack_store(kv_cache[:Np])
8:   kv_cache_pack.update(kv_pack)
9:   kv_cache_residual.update(kv_cache[-res_len:])
10:  return kv_cache_pack, kv_cache_residual, res_len
11: end function
12: function DECODE
13:   Input: Q, K, V, kv_cache_residual, kv_cache_pack,
    res_len
14:   res_len ← res_len + 1
15:   kv_cache_residual.update(K, V)
16:   Ores, Kpack_new, Vpack_new ←
    RESIDUALKERNEL(Q, kv_cache_residual, res_len, Nr)
17:   Omain ← PACKINGKERNEL(Q, kv_cache_pack)
18:   Ofinal ← COMBINEKERNEL(Ores, Omain)
19:   % 3. Cache Update Phase
20:   if res_len = Nr then
21:     kv_cache_pack.update(Kpack_new, Vpack_new)
22:     kv_cache_residual.clear()
23:     res_len ← 0
24:   end if
25:   return Ofinal
26: end function
27: function RESIDUALKERNEL
28:   Input: Q, kv_cache_residual, res_len, Nr
29:   Kres, Vres ← kv_cache_residual
30:   % ... After computation ...
31:   if res_len = Nr then
32:     Kpack_new ← qpack_store(Kres)
33:     Vpack_new ← qpack_store(Vres)
34:   end if
35:   return Ores, Kpack_new, Vpack_new
36: end function

```

asynchronous nature of WGMMA overlaps storage with computation, optimizing performance.

4.2 Warps-Efficient Parallel Dequantization.

Multi-warps Layout for Dequantization. As illustrated in Figure 4b, BitDecoding introduces a novel warp layout to enable parallel dequantization of multiple packed data chunks. Unlike the original warp partitioning strategy, which allocates multiple warps along the M dimension, we first reduce the warp allocation along M to $W_m = 1$ —since the query length is typically less than 16—while increasing the number of warps along the N dimension (W_n).

By increasing the number of warps along N dimension, the stalls introduced by dequantization operations can be mitigated by the Streaming Multiprocessor (SM) warp scheduler [24], effectively improving parallelism. Additionally, the computational loop depth is reduced by a factor of W_n , further enhancing efficiency.

Under the PTX instruction `mma.m16n8k16`, the warp iteration count along the N dimension follows:

$$\text{Iteration Count} = \frac{T_n}{W_n \times 8} \quad (7)$$

where W_n warps concurrently execute dequantization on packed data before performing matrix multiplication using Tensor Cores.

While the whole number of warps is influenced by the overall attention mechanism due to additional register allocation, we adhere to the configuration used in FlashAttention where $W_n = W_{total}$.

Multi-warps Cooperative Softmax. With a multi-warps layout design, BitDecoding distributes the workload across warps to compute partial attention scores ($S = QK^T$). However, since results are spread across different registers and warps, the original register-level softmax is no longer viable.

To address this, we introduce a small shared memory buffer, *sTMP* (size W_n), enabling cross-warp reduction and synchronization.

A key challenge then arises due to the warp layout incompatibility with the subsequent MMA computation for *PV*. To resolve this, we allocate a shared memory buffer, *sAcc* (T_m, T_n), to temporarily store *P* before loading it via `ldmatrix`, ensuring proper Tensor Core alignment (see Algorithm 3).

Since W_n is small, we reuse *sTMP*'s shared memory pointer for *sAcc*, minimizing overhead. Additionally, on Hopper Tensor Cores, WGMMA can read from shared memory directly, eliminating the need for explicit loading instructions.

Algorithm 3 Multi-warps Cooperative Softmax

Require: $sTMP \in \mathbb{R}^{W_n}$ and $sAcc \in \mathbb{R}^{T_m \times T_n}$ in SMEM.

Require: Load $Q_i \in \mathbb{R}^{T_m \times d}$ and $K_i, V_i \in \mathbb{R}^{T_n \times d}$ to REG.

- 1: $S_i = Q_i K_j^T$ where $S_i \in \mathbb{R}^{T_m \times T_n}$.
 - 2: $m_i^{new} = \max(m_i, \text{rowmax}(S_i, sTMP))$.
 - 3: $P_i = \exp(S_i - m_i^{new})$ where $P_i \in \mathbb{R}^{T_m \times T_n}$.
 - 4: $sAcc = \text{tiled_copy_r2s}(P_i)$.
 - 5: $P'_i = \text{tiled_copy_s2r}(sAcc)$.
 - 6: $O_i^{new} = P'_i V_j + \text{diag}(e^{m_i - m_i^{new}}) O_i$.
-

4.3 Asynchronous Pipeline Design

Low-bit kv cache decoding kernel introduces additional overhead due to the need to load quantization parameters (scales and zeros) and perform dequantization on CUDA cores. To mitigate this, we design a fine-grained asynchronous pipeline

optimized for mixed-precision attention computation, as illustrated in Figure 9.

Global to Shared Memory. To efficiently manage quantization parameters, we introduce dedicated shared memory buffers for quantization parameter K_{pack} params (K_p) and V_{pack} param (V_p), facilitating efficient tiling for memory copy. These buffers store scale and zeros in the half2 format, allowing them to be loaded in a single instruction.

The shape of K_p is determined by the quantization granularity setting, and the V_p follows a Token-wise layout:

- **Channel-wise:** $(T_n/\text{group_size}, d)$.
- **Token-wise:** $(T_n, d/\text{group_size})$.

To achieve optimal memory overlapping, all global-to-shared memory transfers are executed asynchronously using the `cp.async` intrinsic, ensuring efficient pipeline execution.

We optimize memory transactions using instruction with different caching strategies:

- **cp.async.cg:** Used for Q, K_{pack} , and V_{pack} , which cache only in global memory as they are not reused within the same kernel.
- **cp.async.ca:** Applied to K_p and V_p , ensuring smaller byte-level alignment for fine-grained memory access.

In Hopper architecture, we follow FA3, leveraging the `tma.copy` instruction for data loading. This facilitates warp-specialized scheduling, improving data locality and reducing memory latency across multiple warps.

Shared Memory to Register. We use the PTX instruction `ldmatrix` to efficiently load K_{pack}, V_{pack} and $sAcc$ from shared memory into registers with the Tensor Cores tiling layout. To eliminate bank conflicts, we use a sizzling scheme [5] defined as:

$$\text{col}_{id} = \text{row}_{id} \oplus \text{col}_{id} \quad (8)$$

achieve bank conflict-free access. Additionally, we restructure the shared memory layout of K_p and V_p to further reduce bank conflict and maximize throughput efficiency.

Computation. To fully utilize both CUDA Cores and Tensor Cores, we design a register-level software pipeline that enables efficient overlapping of computation and memory operations. In this pipeline, shared memory reads via `ldmatrix` and dequantization operations (`Dequant`) are executed concurrently with Tensor Core matrix multiplications (`MMA`) under the warp scheduler of Streaming Multiprocessors (SMs).

Specifically, while the i_{th} slice is being processed by MMA instructions in Tensor Cores, the $(i+1)_{th}$ slice is simultaneously loaded from shared memory via `ldmatrix` and undergoes dequantization. This design ensures continuous data flow, thereby improving instruction throughput and maximizing hardware utilization.

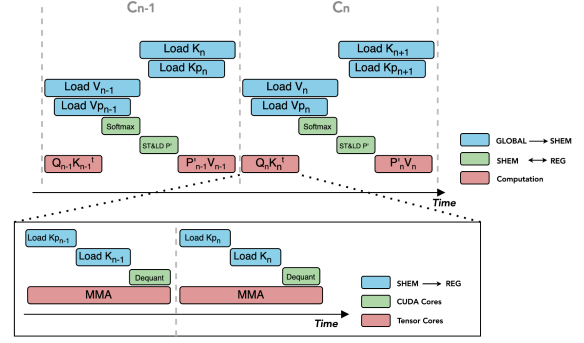


Figure 9. Software pipeline of mix-precision decoding.

5 Evaluation

We evaluate the performance at two levels: kernel-level benchmark using the *Packing kernel* with different GPU architectures and model-level end-to-end LLMs inference with different LLMs model including LLaMA-2-7B (MHA) and LLaMA-3.1-8B (GQA) by using Transformers library [33]. For our ablation study, we employ NVIDIA Nsight Compute [21] to perform low-level microbenchmarking.

Implementation. The GPU Kernel is implemented by extending the FlashAttention kernel using CUDA, PTX instruction, Nvidia’s CUTLASS library [5], and TileLang [1]. It is designed as a modular, plug-and-play PyTorch plugin, allowing integration with the FlashAttention API at the PyTorch level.

System setup. To evaluate the experimental performance across diverse GPU architecture, we conducted experiments under the following hardware configurations:

- **Ampere (SM80):** AMD EPYC 7V13 CPU with NVIDIA A100 80GB PCIE GPU, running CUDA 12.3.
- **Ada Lovelace (SM89):** AMD EPYC 7402 CPU with NVIDIA RTX 4090 GPU, running CUDA 12.2.
- **Hopper (SM90):** AMD EPYC 9554 CPU with NVIDIA H100 80GB HBM3 GPU, running CUDA 12.4.

5.1 Kernel Performance Comparison

Workloads. We evaluate the performance of the *Packing Kernel* across different serving scenarios:

- **Single:** A scenario where `batch_size = 1`, representing inference for edge users.
- **Batches:** A setting with a larger `batch_size`, maintaining the same input length while applying simple padding.
- **Page:** A high-throughput scenario where a larger `batch_size` is managed using the page management technique [16].

Additionally, we analyze the impact of different head configurations for both MHA and GQA. The first row in our

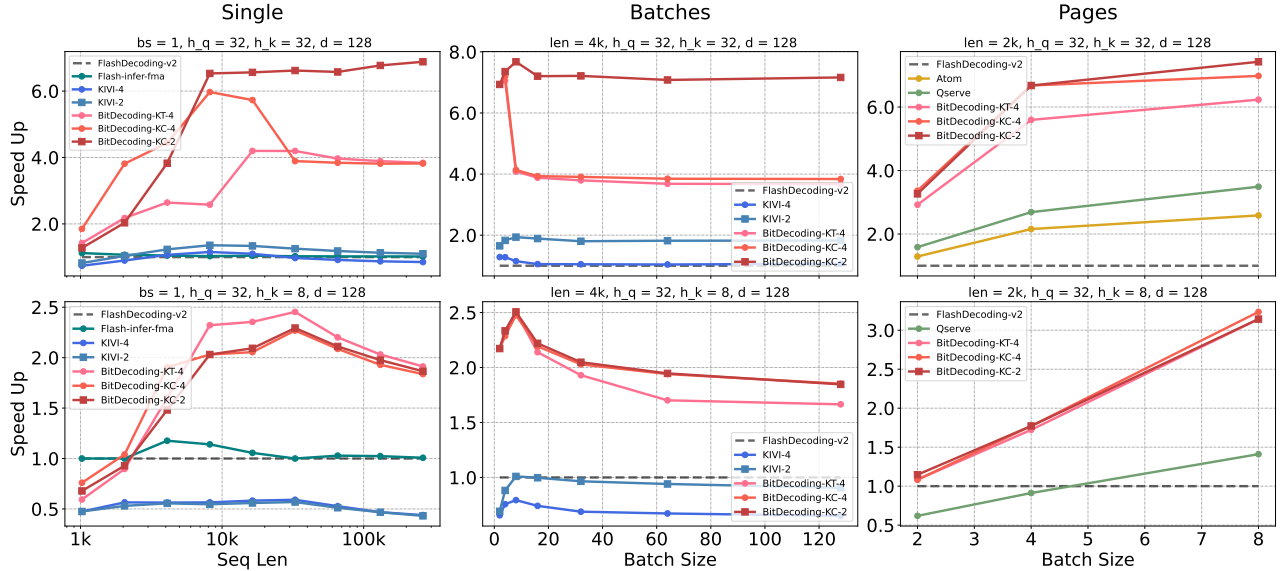


Figure 10. Kernel performance on RTX4090.

results corresponds to MHA settings, while the second row represents GQA where $n_{group} > 1$.

For kernel comparison on Hopper, we set $q_{len} = 4$ since FlashDecoding-3 demonstrates a significant speedup in speculative decoding [17] while maintaining the same performance as v2 when $q_{len} = 1$.

Baselines. We compare BitDecoding against several kernel implementations, including FlashDecoding [6, 25], the split partitioning version of FlashAttention optimized for long-context; FlashInfer [35] a customizable attention Kernels library; KIVI [19], a widely used method integrated into the Transformers library, supports both 4-bit and 2-bit quantization. Additionally, we evaluate Atom [37] and QServe [18], two serving system implementations that support 4-bit KV cache with page management. Notably, Atom does not support the GQA variant.

Results on RTX4090. As shown in Figure 10, under Single and Batches serving settings, BitDecoding-4bit achieves roughly $4\times$ speedup over FlashDecoding-v2, with the 2-bit implementation exceeding $7\times$. This significant improvement comes from its low-bit KV Cache, alleviating memory bottlenecks due to limited DRAM bandwidth on the RTX 4090. Notably, the 4-bit kernel shows particularly high gains at smaller KV Cache sizes before stabilizing around $4\times$, highlighting BitDecoding’s superior parallelism and computational efficiency compared to FlashAttention. In contrast, KIVI, implemented in PyTorch and Triton with separate kernel launches, suffers performance loss due to inefficient memory patterns and lack of kernel fusion.

Under the Pages setting, BitDecoding consistently surpasses QServe and Atom by more than $2\times$ in MHA. QServe’s

performance degrades under the GQA setting, as it relies on CUDA cores instead of Tensor Cores.

Results on A100. As shown in Figure 11, BitDecoding achieves roughly $3\times$ speedup, with greater improvements for longer sequences and larger KV Cache sizes. Due to higher DRAM bandwidth on A100, the gap between 4-bit and 2-bit implementations narrows. Since computation dominates execution time on A100, methods not utilizing Tensor Cores see performance declines, especially under GQA. Specifically, under the Pages workload, BitDecoding attains over $2.5\times$ speedup, while QServe achieves only $0.5\times$.

Results on H100. As illustrated in Figure 12, Decoding-v3, optimized for Hopper Tensor Cores, achieves notable performance improvements over its v2 counterpart. BitDecoding demonstrates significant speedups across both Single and Batches workloads. While BitDecoding-v2 achieves up to $1.7\times$ and $4.1\times$ speedup in single-query and batched settings, respectively, leveraging Hopper Tensor Cores in v3 further amplifies these gains, reaching up to $3.5\times$ speedup in the single scenario and an impressive $9.0\times$ in the batches setting.

5.2 End-to-end LLM Inference

Workloads. We evaluate the end-to-end inference performance of BitDecoding in A100 on LLMs, LLaMA-2-7B (MHA) and LLaMA-3.1-8B (GQA). We measure the average latency of generating one token and the throughput in the decode stage under different sequence lengths and token budgets. We choose channel-wise quantization as it brings better accuracy and aligns with the KIVI.

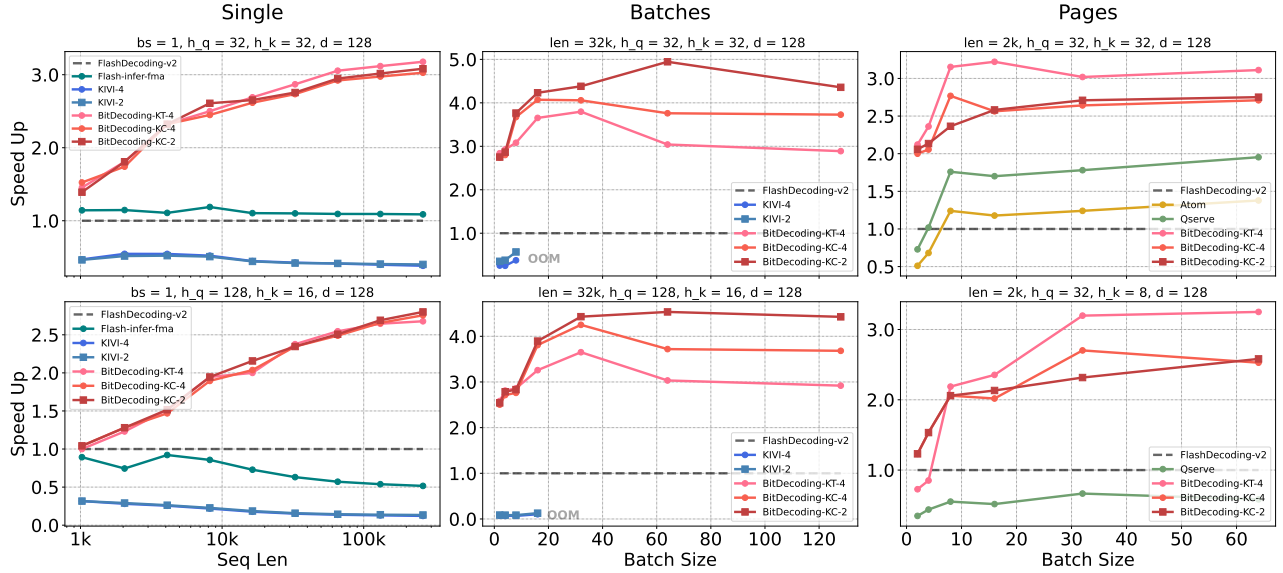


Figure 11. Kernel performance on A100.

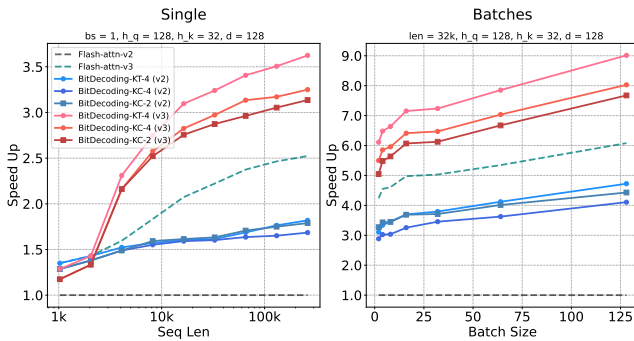


Figure 12. Kernel performance on H100.

Single and Batches Serving. As illustrated in Figure 13, in the Single setting, BitDecoding achieves up to 3.3× speedup at a 128K context length, where KV cache loading becomes the primary bottleneck in LLM inference. In contrast, KIVI encounters out-of-memory (OOM) issues as it lacks support for block tiling kernel implementations.

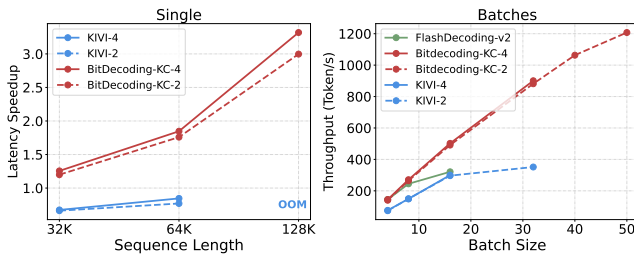


Figure 13. Performance comparison for Llama3.1-8B. The batches setting is under $seq_len = 4K$.

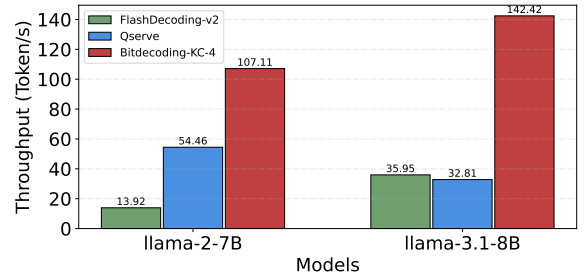


Figure 14. Performance comparison with page setting. The batches setting is under $seq_len = 32K$.

For Batches, BitDecoding demonstrates significant throughput improvements due to its reduced bit-width. The 2-bit variant achieves up to 1200 tokens/s, while the 4-bit variant reaches 900 tokens/s—both substantially outperforming the baseline FlashDecoding-v2, which remains below 300 tokens/s.

Page serving. We compare BitDecoding with QServe for page-setting inference, as QServe supports both MHA and GQA attention structures. The maximum throughput is evaluated under the largest batch sizes available within GPU memory. As illustrated in Figure 14, QServe achieves higher throughput than FlashDecoding-v2 on LLaMA-2-7B but suffers from degraded performance on LLaMA-3.1-8B due to inefficiencies in handling GQA. In contrast, BitDecoding demonstrates superior performance across both LLaMA architectures, achieving more than 2× higher maximum throughput compared to QServe and FlashDecoding-v2.

Efficiency and Accuracy Trade Off. As shown in Table 2, we evaluate throughput and accuracy across different bit widths. The 2-bit quantization reduces memory consumption significantly, enabling larger batch sizes and achieving a $4.25\times$ higher throughput compared to FP16. Meanwhile, the 4-bit quantization achieves a $2.98\times$ speedup while maintaining near full-precision accuracy with only a minimal 0.2% degradation. These results highlight the trade-off, with 4-bit quantization offering balance and 2-bit maximizing throughput at a slight accuracy cost.

Table 2. Efficiency and accuracy tradeoff with low-bit KV cache. We use Llama-3.1-8B with $seq_len = 32K$, and evaluate average accuracy on longbench [3]

KV Cache	Throughput	Accuracy
FP16	49.25	48.25
INT4	147.21 (+2.98x)	48.16 (-0.2%)
INT2	209.48 (+4.25x)	47.38 (-2.7%)

5.3 Analysis and Ablation Study

Quantization and Packing Overhead. We measure the time required for quantization and packing under $seq_len = 128k$. For comparison, we use Flute [11], an existing implementation that performs pre-transformation using PyTorch.

As shown in Table 3, the pre-transformation and packing step (Pack_torch) in previous mixed-precision computing methods introduce significant overhead, which cannot be ignored. Our Qpack kernel incurs minimal overhead after the Prefill phase, primarily due to kernel launch overhead. In contrast, Qpack_fusion achieves nearly negligible overhead, as it is fully fused into kernel computation.

Table 3. Latency (ms) comparison of different quantization and packing methods.

Quantization	Pack_torch	Qpack	Qpack_fusion
4bit	1.163	0.0599	0.008
2bit	-	0.1114	0.009

Dequantization Overhead. Figure 15 illustrates the high computational overhead of dequantization in Atom and QServe, consuming nearly half the kernel execution time. In contrast, BitDecoding significantly reduces this overhead to less than 15% (4-bit) and 35% (2-bit), thanks to better Tensor Core overlap.

A further microbenchmark comparing Atom and BitDecoding (Figure 15b) reveals BitDecoding’s superior memory throughput from effective Tensor Core usage. Conversely, Atom relies heavily on CUDA cores, increasing pressure on FMA and ALU operations.

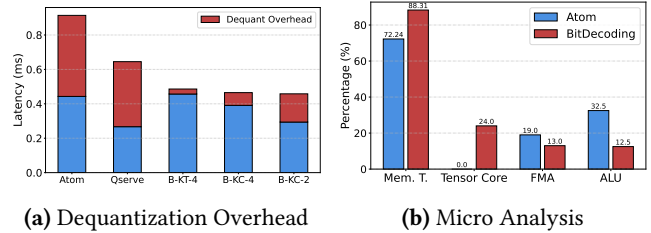


Figure 15. Dequantization overhead analysis.

BreakDown Analysis. To further analyze the performance gains of BitDecoding, we decompose our optimizations in Table 4. The Lop3 tensor core mapping and the asynchronous pipeline contribute to a $1.2\times$ – $1.5\times$ speedup, while the warp-efficient design achieves more than $2\times$ speedup by enhancing overall computational parallelism.

Table 4. Latency (ms) performance with breakdown optimizations.

Optimizations			Seq Len		
Lop3	Warp	Async	32K	64K	128K
✓	✓	✓	0.16	0.31	0.61
✓	-	✓	0.26	0.50	0.88
-	✓	✓	0.47	0.85	1.63
✓	✓	-	0.29	0.53	1.09
-	-	-	0.58	1.08	2.13

6 Related Works

KV Cache Quantization Algorithms. KV cache quantization reduces memory usage in LLMs with long contexts while maintaining performance. Recent works explore 4-bit, 2-bit, and even 1-bit KV cache quantization, aiming to push the limits of compression. Methods like KIVI [19], Gear [14], and KVQuant [12] use per-channel quantization to handle key-value outliers, while RotateKV [27] applies rotation to smooth channel-wise distributions. Although effective at higher compression ratios, these methods lack efficient system implementations, leading to suboptimal performance.

Mixed-precision Matrix Multiplication. Low-bit weight and low-bit KV cache in LLMs create a unique requirement for mixed-precision matrix multiplication (mpGEMM), where one input matrix is in lower precision (e.g., INT4/2/1) while the other matrix remains in higher precision (e.g., FP16/8). Optimized kernels like Ladder [32] and Marlin [9] improve performance via layout transformations and efficient dequantization. However, these methods require pre-packing and pre-transforming weights, limiting applicability to low-bit KV cache in autoregressive decoding.

System Implementation for Low-bit KV Cache. KIVI [30] uses Triton with separate kernels for low-bit KV Cache implementation. Atom [37] integrates quantization within the

preceding linear layer, while QServe [18] fuses quantization directly into FlashAttention kernels. However, they both rely on GEMV operations with fused multiply-add (FMA) instructions, missing Tensor Core acceleration. TurboAttention [13] utilizes INT8 Tensor Cores without specialized optimizations, providing modest speedup over QServe.

7 Conclusion

In this paper, we introduce BitDecoding, a GPU-optimized computing framework supporting low-bit KV cache decoding with Tensor Cores. We tackle the problem of layout mismatch incurred by Tensor Core’s rigid computation patterns and propose fine-grained optimizations for higher computational utilization. Extensive evaluations across multiple GPU architectures demonstrate that BitDecoding achieves up to 7.5× speedup on RTX 4090, 4.8× on A100, and 8.9× on H100 compared to FP16 FlashDecoding. Furthermore, on LLaMA-3.1-8B with a 128K sequence length, BitDecoding reduces single-batch decoding latency by 3× and achieves a 4× improvement in serving throughput over state-of-the-art methods.

References

- [1] Tile AI. 2025. TileLang: A Domain-Specific Language for Efficient ML Compilation. <https://github.com/tile-ai/tilelang> Accessed: 2025-03-12.
- [2] Joshua Ainslie, James Lee-Thorp, Michiel De Jong, Yury Zemlyanskiy, Federico Lebrón, and Sumit Sanghani. 2023. Gqa: Training generalized multi-query transformer models from multi-head checkpoints. *arXiv preprint arXiv:2305.13245* (2023).
- [3] Yushi Bai, Xin Lv, Jiajie Zhang, Hongchang Lyu, Jiankai Tang, Zhidian Huang, Zhengxiao Du, Xiao Liu, Aohan Zeng, Lei Hou, Yuxiao Dong, Jie Tang, and Juanzi Li. 2024. LongBench: A Bilingual, Multitask Benchmark for Long Context Understanding. In *Proceedings of the 62nd Annual Meeting of the Association for Computational Linguistics (Volume 1: Long Papers)*. Association for Computational Linguistics, Bangkok, Thailand, 3119–3137. doi:10.18653/v1/2024.acl-long.172
- [4] Yapei Chang, Kyle Lo, Tanya Goyal, and Mohit Iyyer. 2023. Boookscore: A systematic exploration of book-length summarization in the era of llms. *arXiv preprint arXiv:2310.00785* (2023).
- [5] NVIDIA Corporation. 2024. CUTLASS: CUDA Templates for Linear Algebra Subroutines and Solvers. <https://github.com/NVIDIA/cutlass> 3.6).
- [6] Tri Dao. 2024. FlashAttention-2: Faster Attention with Better Parallelism and Work Partitioning. In *International Conference on Learning Representations (ICLR)*.
- [7] Tri Dao, Daniel Haziza, Francisco Massa, and Grigory Sizov. 2023. Flash-Decoding for long-context inference. <https://crfm.stanford.edu/2023/10/12/flashdecoding.html> Accessed: 2025-03-10.
- [8] Yiran Ding, Li Lyna Zhang, Chengruidong Zhang, Yuanyan Xu, Ning Shang, Jiahang Xu, Fan Yang, and Mao Yang. 2024. Longrope: Extending llm context window beyond 2 million tokens. *arXiv preprint arXiv:2402.13753* (2024).
- [9] Elias Frantar, Roberto L. Castro, Jiale Chen, Torsten Hoefler, and Dan Alistarh. 2024. Marlin: Mixed-precision auto-regressive parallel inference on large language models. *arXiv preprint arXiv:2408.11743* (2024).
- [10] Daya Guo, Dejian Yang, Haowei Zhang, Junxiao Song, Ruoyu Zhang, Runxin Xu, Qihao Zhu, Shirong Ma, Peiyi Wang, Xiao Bi, et al. 2025. Deepseek-r1: Incentivizing reasoning capability in llms via reinforcement learning. *arXiv preprint arXiv:2501.12948* (2025).
- [11] Han Guo, William Brandon, Radostin Cholakov, Jonathan Ragan-Kelley, Eric Xing, and Yoon Kim. 2024. Fast Matrix Multiplications for Lookup Table-Quantized LLMs. In *Findings of the Association for Computational Linguistics: EMNLP 2024*. 12419–12433.
- [12] Coleman Hooper, Sehoon Kim, Hiva Mohammadzadeh, Michael W Mahoney, Yakun Sophia Shao, Kurt Keutzer, and Amir Gholami. 2024. Kvquant: Towards 10 million context length llm inference with kv cache quantization. *arXiv preprint arXiv:2401.18079* (2024).
- [13] Hao Kang, Srikant Bharadwaj, James Hensman, Tushar Krishna, Victor Ruhle, and Saravan Rajmohan. 2024. TURBOATTENTION: Efficient Attention Approximation For High Throughputs LLMs. *arXiv preprint arXiv:2412.08585* (2024).
- [14] Hao Kang, Qingru Zhang, Souvik Kundu, Geonhwa Jeong, Zaoxing Liu, Tushar Krishna, and Tuo Zhao. 2024. Gear: An efficient kv cache compression recipe for near-lossless generative inference of llm. *arXiv preprint arXiv:2403.05527* (2024).
- [15] Young Jin Kim, Rawn Henry, Raffy Fahim, and Hany Hassan Awadalla. 2022. Who Says Elephants Can’t Run: Bringing Large Scale MoE Models into Cloud Scale Production. *arXiv preprint arXiv:2211.10017* (2022).
- [16] Woosuk Kwon, Zhuohan Li, Siyuan Zhuang, Ying Sheng, Lianmin Zheng, Cody Hao Yu, Joseph E. Gonzalez, Hao Zhang, and Ion Stoica. 2023. Efficient Memory Management for Large Language Model Serving with PagedAttention. In *Proceedings of the 29th ACM Symposium on Operating Systems Principles*. doi:10.1145/3600006.3613165
- [17] Yaniv Leviathan, Matan Kalman, and Yossi Matias. 2023. Fast Inference from Transformers via Speculative Decoding. In *International Conference on Machine Learning (ICML)*. PMLR. <https://arxiv.org/pdf/2211.17192>
- [18] Yujun Lin, Haotian Tang, Shang Yang, Zhekai Zhang, Guangxuan Xiao, Chuang Gan, and Song Han. 2024. Qserve: W4a8kv4 quantization and system co-design for efficient llm serving. *arXiv preprint arXiv:2405.04532* (2024).
- [19] Zirui Liu, Jiayi Yuan, Hongye Jin, Shaochen Zhong, Zhaozhuo Xu, Vladimir Braverman, Beidi Chen, and Xia Hu. 2024. Kivi: A tuning-free asymmetric 2bit quantization for kv cache. *arXiv preprint arXiv:2402.02750* (2024).
- [20] Weile Luo, Ruibo Fan, Zeyu Li, Dayou Du, Qiang Wang, and Xiaowen Chu. 2024. Benchmarking and dissecting the nvidia hopper gpu architecture. *arXiv preprint arXiv:2402.13499* (2024).
- [21] NVIDIA Corporation. 2025. Nsight Compute - Get Started. <https://developer.nvidia.com/tools-overview/nsight-compute/get-started> Accessed: 2025-03-11.
- [22] OpenAI. 2025. OpenAI o3-mini. <https://openai.com/index/openai-o3-mini/> Accessed: 2025-02-14.
- [23] Bowen Peng, Jeffrey Quesnelle, Honglu Fan, and Enrico Shippole. 2023. Yarn: Efficient context window extension of large language models. *arXiv preprint arXiv:2309.00071* (2023).
- [24] Suhel Shah, Fathy Essa, and Mai Fadel. 2015. A survey of techniques for warp scheduling in GPUs. In *2015 IEEE Seventh International Conference on Intelligent Computing and Information Systems (ICICIS)*. IEEE, 600–606.
- [25] Jay Shah, Ganesh Bikshandi, Ying Zhang, Vijay Thakkar, Pradeep Ramani, and Tri Dao. 2024. Flashattention-3: Fast and accurate attention with asynchrony and low-precision. *Advances in Neural Information Processing Systems* 37 (2024), 68658–68685.
- [26] Noam Shazeer. 2019. Fast transformer decoding: One write-head is all you need. *arXiv preprint arXiv:1911.02150* (2019).
- [27] Zunhai Su, Zhe Chen, Wang Shen, Hanyu Wei, Ling Li, Huangqi Yu, and Kehong Yuan. 2025. RotateKV: Accurate and Robust 2-Bit KV Cache Quantization for LLMs via Outlier-Aware Adaptive Rotations. *arXiv preprint arXiv:2501.16383* (2025).

- [28] Qian Tao, Wenyuan Yu, and Jingren Zhou. 2024. Asymkv: Enabling 1-bit quantization of kv cache with layer-wise asymmetric quantization configurations. *arXiv preprint arXiv:2410.13212* (2024).
- [29] Gemini Team, Petko Georgiev, Ving Ian Lei, Ryan Burnell, Libin Bai, Anmol Gulati, Garrett Tanzer, Damien Vincent, Zhufeng Pan, Shibo Wang, et al. 2024. Gemini 1.5: Unlocking multimodal understanding across millions of tokens of context. *arXiv preprint arXiv:2403.05530* (2024).
- [30] Philippe Tillet, Hsiang-Tsung Kung, and David Cox. 2019. Triton: an intermediate language and compiler for tiled neural network computations. In *Proceedings of the 3rd ACM SIGPLAN International Workshop on Machine Learning and Programming Languages*. 10–19.
- [31] Ashish Vaswani, Noam Shazeer, Niki Parmar, Jakob Uszkoreit, Llion Jones, Aidan N. Gomez, Lukasz Kaiser, and Illia Polosukhin. 2017. Attention Is All You Need. In *Advances in Neural Information Processing Systems*, Vol. 30. 5998–6008. <https://arxiv.org/abs/1706.03762>
- [32] Lei Wang, Lingxiao Ma, Shijie Cao, Quanlu Zhang, Jilong Xue, Yining Shi, Ningxin Zheng, Ziming Miao, Fan Yang, Ting Cao, et al. 2024. Ladder: Enabling Efficient {Low-Precision} Deep Learning Computing through Hardware-aware Tensor Transformation. In *18th USENIX Symposium on Operating Systems Design and Implementation (OSDI 24)*. 307–323.
- [33] Thomas Wolf, Lysandre Debut, Victor Sanh, Julien Chaumond, Clement Delangue, Anthony Moi, Pierric Cistac, Tim Rault, Rémi Louf, Morgan Funtowicz, and Jamie Brew. 2020. Transformers: State-of-the-Art Natural Language Processing. arXiv:1910.03771 [cs.CL] <https://github.com/huggingface/transformers>
- [34] Xiaocui Yang, Wenfang Wu, Shi Feng, Ming Wang, Daling Wang, Yang Li, Qi Sun, Yifei Zhang, Xiaoming Fu, and Soujanya Poria. 2023. MM-BigBench: Evaluating Multimodal Models on Multimodal Content Comprehension Tasks. *arXiv preprint arXiv:2310.09036* (2023).
- [35] Zihao Ye, Lequn Chen, Ruihang Lai, Wuwei Lin, Yineng Zhang, Stephanie Wang, Tianqi Chen, Baris Kasikci, Vinod Grover, Arvind Krishnamurthy, and Luis Ceze. 2025. FlashInfer: Efficient and Customizable Attention Engine for LLM Inference Serving. *arXiv preprint arXiv:2501.01005* (2025). <https://arxiv.org/abs/2501.01005>
- [36] Tianyi Zhang, Jonah Yi, Zhaozhuo Xu, and Anshumali Shrivastava. 2024. Kv cache is 1 bit per channel: Efficient large language model inference with coupled quantization. *Advances in Neural Information Processing Systems* 37 (2024), 3304–3331.
- [37] Yilong Zhao, Chien-Yu Lin, Kan Zhu, Zihao Ye, Lequn Chen, Size Zheng, Luis Ceze, Arvind Krishnamurthy, Tianqi Chen, and Baris Kasikci. 2024. Atom: Low-bit quantization for efficient and accurate llm serving. *Proceedings of Machine Learning and Systems* 6 (2024), 196–209.